AEROSOL CHARACTERIZATION BASED ON CHEMICAL COMPOSITION AND OPTICAL PROPERTIES

L. MARMUREANU, J. VASILESCU, A. NEMUC, D. NICOLAE and L. BELEGANTE

National Institute of Research and Development for Optoelectronics, Măgurele, 077125, Romania
E-mails: mluminita@inoe.ro, jeni@inoe.ro (corresponding author), anca@inoe.ro, nnicol@inoe.ro, belegantelivio@inoe.ro

Received April 11, 2016

The aerosols generated by a local fire and their oxidation process in the atmosphere have been studied. The Aerosol Mass Spectrometer was used to identify the oxidation level of organic aerosols, their possible source and the presence of m/z 44, 43, 55, 57 ions. The scattering coefficients of the aerosols were retrieved from the Nephelometer (Model 3563) data. The 450 nm scattering coefficient was analyzed in relation to different types of chemical species like SO_4, Chl or NH_4 and also for total organics or specific ions. The resolved organic spectra through source apportionment analyses pin pointed the dependence between scatter and freshly emitted organics aerosols.

Key words: organic aerosols, mass spectrometry, scattering coefficient.

1. INTRODUCTION

Aerosol is defined as a colloid suspension of fine solid particles or liquid droplets in a gas [1] and is classified depending on the size of the particles ranging between 0.3 and 10 μm [2].

The level of scientific understanding related to aerosols properties and behavior is medium and low, respectively [3]. The estimation of optical parameters contains uncertainties related to the emission sources, mixing and separation from natural background aerosol, state of mixing, method of mixing and asphericity [3].

Human activities represent one of the most important sources for aerosol particles and gases that influence the secondary aerosol formation. From the total amount of fine particulate matter (PM) mass approximately 50% is represented by organic components [4].

The aerosols effect on the local environment can be assessed after identification of the chemical and physical properties of the particles, as well as their concentrations. Rapid change of aerosol's physical and chemical properties represents a barrier in the assessment of aerosol radiative forcing [5].

Some processes like coagulation, gas-particle transformation or aging through oxidation lead to changes in particle size, structure and chemical composition [2]. Measurement of the chemical composition and of the optical properties of atmospheric particles is a significant analytical challenge: just one single aerosol particle is formed from hundreds of molecules as some authors [2, 6] concluded. To date, no single method exists to achieve this task, but spectrometry and light scattering combined can give more details about particle concentration, size distribution, chemical composition, refractive index and internal mixture of aerosols among other properties.

Light scattering depends on a number of factors such as particle size, chemical composition and density. From previous studies, urban aerosols is characterised by more absorbing properties (due to elemental carbon presence as a result of combustion sources) since remote aerosol have more scattering properties [7]. Also $(NH_4)_2SO_4$, NH_4NO_3 and organic matter have been proved to be the dominant species contributing to light scatter under both dry and ambient conditions by several studies made in Beijing under different pollution levels [8]. The available literature [9, 10] shows that the direct comparison between Nephelometer scattering coefficient and Aerosol Mass Spectrometer (AMS) mass concentration reveals a strong correlation. Thus detailed analysis of ion fragments can provide more information about the internal structure of the aerosols.

The main aim of the present study is to analyse the relation between some inorganic ion fragments, submicronic primary or secondary organic aerosol [1, 4] as contributors to light scattering, using two state of the art equipments that measure scatter coefficient of the aerosols and chemical composition of non-refractory PM1 particles.

The paper is organized as follows: Section 2 describes the site, instruments and methodology used in this paper; Section 3 presents the results related to complex analyses of aerosol type and the scattering coefficient, while the last section of the paper present some concluding remarks.

2. EXPERIMENTS

2.1. SITE

The measurements were made in a peri-urban area near Bucharest influenced by traffic, local industry and domestic activity like local fires. Măgurele is a city located at 44.35 N; 26.03 E; ASL 93 m, with a temperate-continental climate [11] Most of the surrounding land is used for agricultural purposes, which can be a source of dust and bio-aerosols [12], since up to 50% of the total amount of atmospheric aerosols originate from land processing. These sources are responsible for coarse mode aerosols. In the studied area, the aerosols are typical for a rural area, with a concentration of less than 50 $\mu g/m^3$ [6]. The PM10 (Particulate Matter with diameter less than 10 μm) trend in Măgurele depends on the season: in spring

the average concentration is 36 μg/m^3, during summer the concentration increases up to 44 μg/m^3 and during autumn decreases to 40 μg/m^3 [13]. During winter the aerosol load can increase up to 80 μg/m^3 but the average value is around 53 μg/m^3, clearly influenced by heating sources [13], behaviour also found in other site locations across Europe [14]. The local pollution is also responsible for secondary aerosols, gaseous precursors being an important source of submicron aerosols, where the main processes are coagulation and condensation [1].

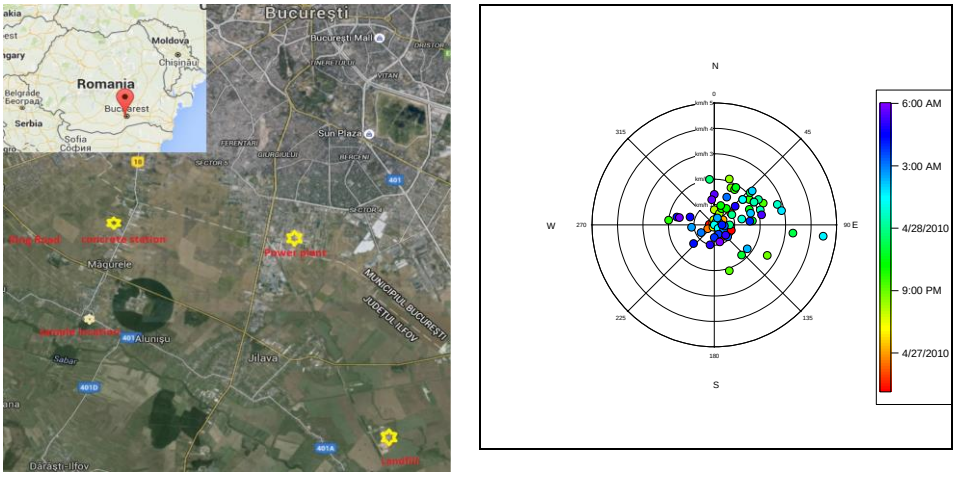

Fig. 1 – Location map and wind rose for measurement period (27–28.04.2010).

It should be noted that approximately 1 km from the sampling site there is a road with relatively high traffic. A power plant (coal and fossil fuel based) located south of Bucharest is an additional source of aerosols and trace gas emissions especially during the winter. A landfill that can be a source of aerosols due to uncontrolled fires is located approximately 8 km from the sampling site. Concrete stations located approximately 3 km from the sampling site can also be significant sources of aerosols (with particles produced from cement processing) (Fig. 1).

2.2. INSTRUMENTS AND METHODOLOGY

The study of aerosols characterisation from chemical and optical point of view is based on two collocated instruments, a C-ToF AMS (Compact-Time of Flight Aerosol Mass Spectrometer) model and Nephelometer (Model 3563). The AMS can be used to determine the mass spectrum and size distribution of aerosols [15], while Nephelometer measure the light scattering of aerosols [16].

Several papers have focused on the operation principles of the C-ToFAMS [17], the sensitivity limits being described in detail by [15]. The C-ToFAMS have the

detection capability ranging from 0.003 μg/m^3 (nitrate, sulphate) to 0.03 μg/m^3 (ammonium, organics).

For these analyses the C-ToF AMS ionizer temperature was set at 600 ^{o}C suitable to efficiently vaporize the volatile ambient particles and aerosols were ionized by electron ionization (70 eV). At this temperature volatile and semivolatile species are vaporized, the instrument not being sensitive to black carbon, sea salt or minerals [18].

C-ToF AMS was periodically calibrated related to ionization efficiency, particle velocity and flow rate. The data processing steps followed the correction procedures (*m*/*z* calibration, baseline subtraction, air beam correction) and were made in Squirrel (SeQUential Igor data RetRiEvaL-Squirrel) software developed in Igor interface [19].

In order to limit the direct contribution of traffic emissions, the AMS sampling tube was positioned above the roof of the building 10 meters above ground level. Samples were taken directly from the environment (without drying the ambient aerosol). Previous experiments by Zelenyuk *et al.* [20] show that the particles lose up to 75% water content, depending on various particularities, when entering in the AMS vacuum system.

The second instrument was a ground-based integrating Nephelometer for continuous monitoring of light scattering coefficient for ambient air. The instrument measures the total scatter and backscatter coefficient on three distinct wavelengths centred on 450, 550 and 700 nm with a 40 nm spectral band [16]. The instrument was placed in the same location as the AMS during the entire experimental procedure, with the air inlet positioned also about 10 m above ground level. The air was collected through a special 37.5 mm tubing designed to minimize aerosol losses due to electrostatic deposition and bending. The line was set up to collect the samples at the same height as the AMS.

Periodic calibrations, according to system requirements, using low and high span gas reference samples (filtered air and CO_2) were carried out to ensure the quality of data. No aerosol drying was performed. The optical parameters retrieved from all channels (scatter and backscatter) were automatically and continuously pre-processed, averaged and stored for further analysis. The acquisition was performed at five minute intervals with automatic noise subtraction every hour for all available data coefficients (scatter and backscatter from the three wavelengths mentioned above).

The environmental parameters (like pressure, temperature and humidity) were important for post-processing and interpretation of data, therefore these parameters were continuously monitored and recorded. Relative humidity was also monitored inside the Nephelometer since various studies emphasized changes in the scatter coefficient with relative humidity inside the instrument (humidity over

50%), lower values being considered for dry air [21]. The average relative humidity fluctuated between 20% and 40% during the measurement period.

Additional environmental parameters (humidity, temperature, wind intensity and direction) were collected using an Environment WM 2000 station. The weather station was collocated with the AMS and the Nephelometer.

For data analyses the mass spectrum data was used, providing information about composition of the aerosol and the mass concentration of several species (organics, sulphate, nitrate, ammonium, chloride). The dimensional distribution of the particles is derived from time of flight signal described by [15]. The C-ToF AMS mass spectrum range is up to mass to charge ratio (*m*/*z)* 800 (that represent the dimensionless quantity resulting from mass number of an ion, divided to its charge number) [22], but the most important ion fragments analysed are: organics (43, 44, 55, 57, 60 and 73), sulphate (48, 64), ammonium (15, 16) and nitrate (30, 46) and chloride (35, 36, 37) [23].

The post processing data analyses was made using Positive Matrix Factorization (PMF) described by [24, 25], performed in Source Finder (SoFi 4.8) integrated software [25]. PMF is described as a matrix equation X = G * F + E. The rows of the matrix F represent the factor profiles, the columns of the matrix G represent the factor time series, since E represent the model residuals.

The organic matrix and errors was calculated in Squirrel software 1.56, applying to the matrixes minimum error of 1 ion, down-weighting the peaks related to CO_2^+ and also *m*/*z* 29 and 30 that are related with air fragmentation. The *m*/*z* 28 was removed to facilitate proper separation of factors.

Data collected from AMS and Nephelometer was averaged during the same time intervals and analysed together using the correlation coefficient.

The scatter coefficient was analysed using Angstrom exponent (1) [26] in order to assess the aerosol size.

Where $\sigma_{\lambda 1}$ and $\sigma_{\lambda 2}$ are the scattering coefficients for the considered wavelengths, and λ_1, λ_2 the wavelengths considered (450 respectively 700 nm).

$$\alpha_{\lambda_1,\lambda_2} = -\frac{\ln\left(\frac{\sigma\lambda_1}{\sigma\lambda_2}\right)}{\ln\left(\frac{\lambda_1}{\lambda_2}\right)}. \quad (1)$$

3. RESULTS AND DISCUSSIONS

In order to highlight some connexions between the aerosol type and the scattering coefficient, we focused on one particular case of aerosols emitted in the atmosphere following the aging process in ambient conditions of organic aerosols. Also the dependencies between scatter coefficient and inorganic species were analysed.

The Nephelometer wavelength used for these comparative measurements was 450 nm, which is sensitive to fine mode aerosols. Particles larger than 50 nm and smaller than 1 μm can be studied based on the Mie scattering theory. According to Kovalev *et al.* [27], the Mie scattering theory is applied for particles with $\rho > 0.03\,\lambda$. For the 450 nm wavelength, the detected particles have a geometric dimension greater than 13.5 nm and maximum detection efficiency at 450 nm.

Analyzed data is summarised in Table 1.

Table 1

List of experiments considered

Case	Date	% organics	% ammonia	% nitrate	% sulphate	% chloride
Fresh emitted aerosols	27.04.2010	48.25	17.22	11.28	17.39	5.86
Oxidized aerosols	28.04.2010	44.93	17.18	13.22	17.26	7.41

The proportions of the most important chemical components are presented for each data set. High chloride and nitrate concentrations were recorded, higher than the annual average. According to Vasilescu *et al.* [28] at this site the most important chemical components of aerosols are organics (~47%), sulfate (~29%) and ammonium (~18%). The nitrate concentration is often very low (3–5%) and chloride is usually only about 1% of the total mass.

Two consecutive days of measurements were performed on April 27th and 28th 2010 using both the AMS and the Nephelometer. On April 27th, a fire occurred near the sampling site and relatively higher concentrations were observed. The fire started during the afternoon and continued for several hours. The evolution and oxidation process of submicron particles were evaluated during the second day of measurement.

Meteorological conditions were characterised the first day by wind direction dominantly from N-E, S-E, with low intensity and average of 1.2 km/h (Fig. 1). Low concentrations of aerosols were observed the second day, characterised by the same wind direction and increased speed up to 4.5 km/h, with an average of 2.18 km/h. The aerosols were quickly spread and the concentration decreased to under 1 μg/m^3 due to the wind speed. The decreasing concentration is in accordance with studies made by Bigi *et al.* [29], where the wind speed is anticorrelated with pollutant concentration.

In both days organic aerosol particles had a contribution more than 40% from the total submicronic mass loadings. Delta pattern-Δ [30] was assessed, in order to identify the type of organic aerosols. Δ was dominated by 0 and 2 series, which are characteristic to alkenes and alkanes [31], with *m*/*z* peaks at 27, 41, 43, 44, 55, 57 (Fig. 2), where

$$\Delta = \frac{m}{z} - 14n + 1. \quad (2)$$

The degree of oxidation of organic particles has been evaluated following the [32] methodology to plot f_{44} *versus* f_{43} [33], which represents the fraction of organic aerosol mass spectrum signal at *m*/*z* 44 and *m*/*z* 43 respectively.

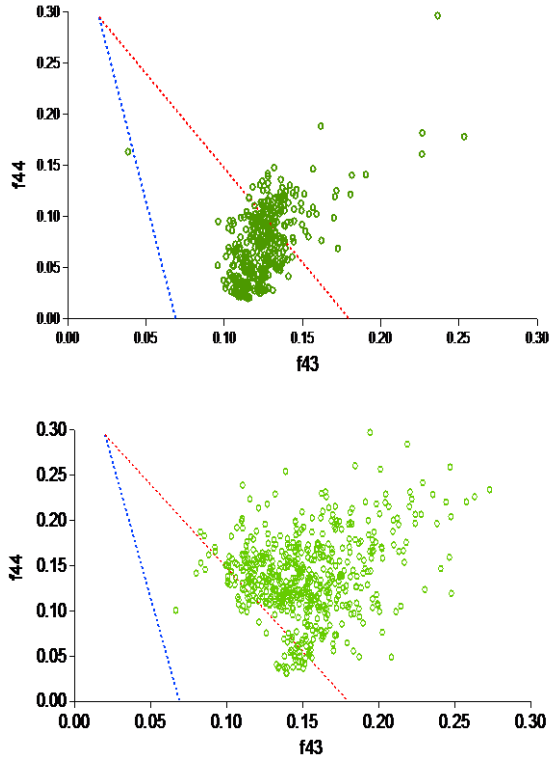

Fig. 2 – Fraction of *m*/*z* 44 to total OA (f_{44}) against the *m*/*z* 43 to total OA (f_{43}) for 27.04.2010 (left panel) and 28.04.2010 (right panel).

During the measurements organic aerosol particles have different characteristics based on f_{44} *vs.* f_{43} signal. During the fire event, f_{44} ranged between 0.02 and 0.2 (Fig. 2, left panel). Lower values than 0.05 is characteristic for freshly emitted aerosol since values higher than 0.05 and less than 0.15 are associated to semi-and low-volatile organic species [34]. For the second day it is evidenced the aging process, the higher values of f_{44} being characteristic for oxidized organics (Fig. 2, right panel).

The organic matter represent one of the most important component identified to be responsible for scatter coefficient, source apportionment analyses highlighted the dependencies between different factors and scatter coefficient. Since local fire

was a particular event, the separation of factors was made considering these 2 days as different events.

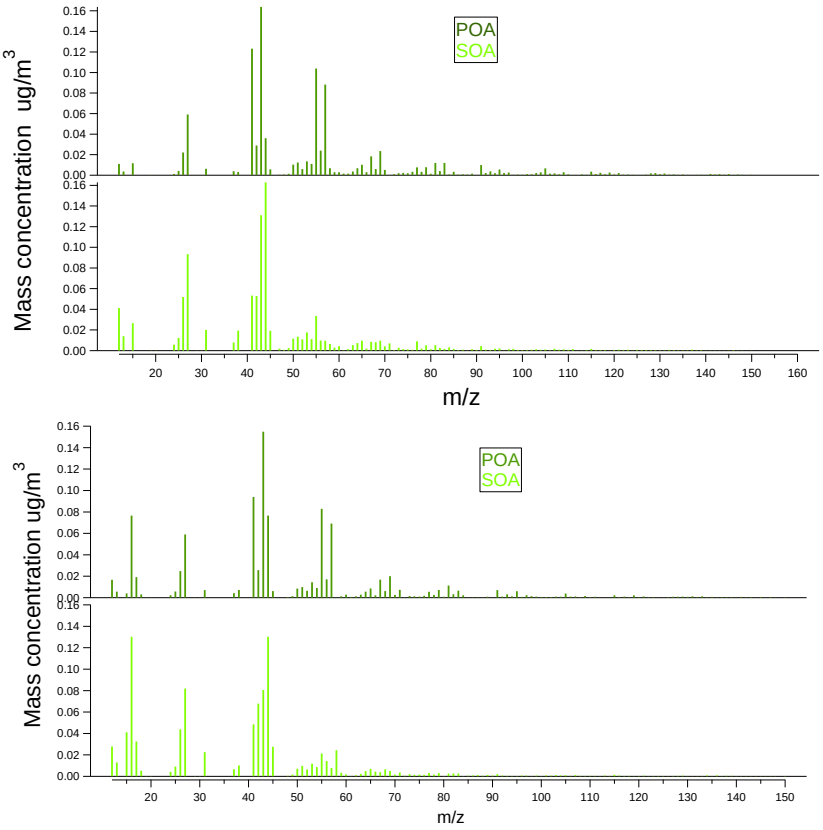

Fig. 3 – Mass spectra of organic aerosols: upper panel – fresh aerosol generated by a local fire; lower panel – aged aerosol in second day.

Two factor solution of PMF analyses is the most appropriate to characterize this event, primary (POA) and secondary organic aerosols (SOA) proportions being assessed. In the first day POA include approximately 71% of the resolved PMF factors, since during the second day of measurements represents only 51% from the total organics. The resolved POA spectra had an important contribution from *m*/*z* 43, *m*/*z* 55 and *m*/*z* 57 ions for both days. A higher concentration of *m*/*z* 44 (mostly CO^{+2}), was confirmed for the second day indicating the presence of oxygenated organic aerosols (OOA) as secondary organic aerosols (SOA) resulted from oxidation of organic compounds.

The correlation coefficient was used to properly compare the scattering properties retrieved using Nephelometer data and the AMS chemical load for the measurements period. The correlation coefficient between chemical species and

scattering coefficient time series showed a high dependence of the scattering coefficient at 450 nm and organics ($r^2 = 0.89$), especially the fresh ones. The correlation coefficient was used to properly compare the scattering properties retrieved using Nephelometer data and the AMS chemical load for the measurements period. The correlation coefficient between chemical species and scattering coefficient time series showed a high dependence of the scattering coefficient at 450 nm and organics ($r^2 = 0.89$), especially the fresh ones. The high dependencies between the species mentioned above and scatter coefficient has been emphasized also by other observations where organic matter represented the most important fraction that influence light scattering in "light polluted" episodes [8].

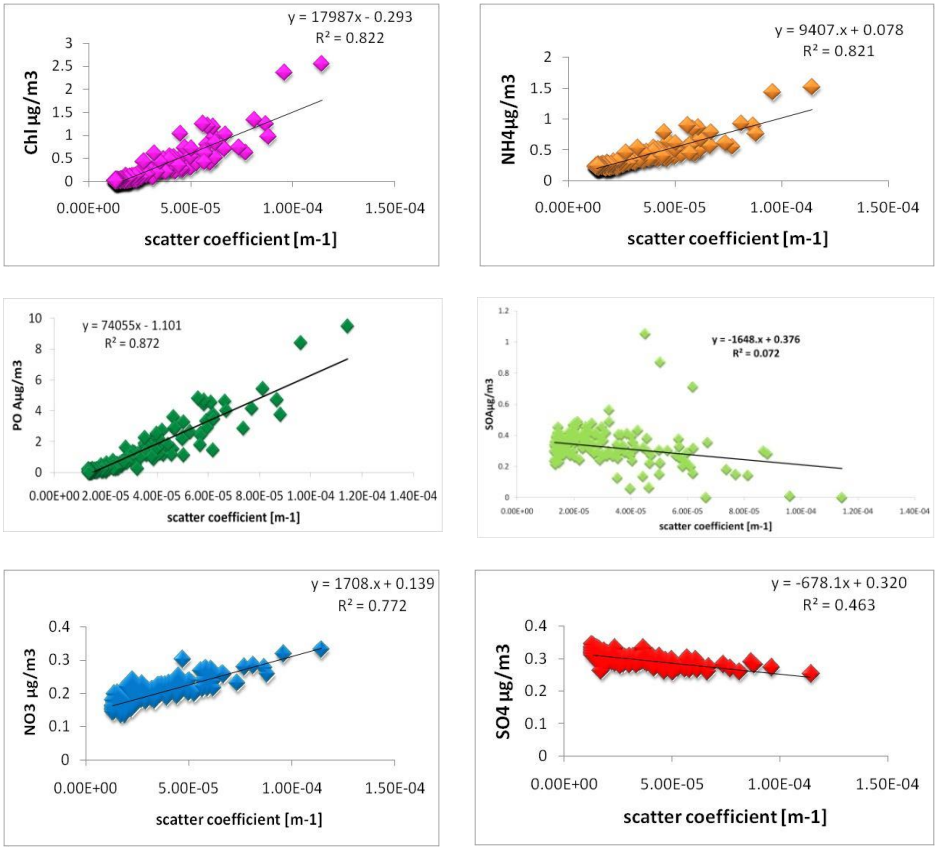

Fig. 4 – Chemical species concentration *vs.* scattering coefficient: upper left panel chloride *vs*. the scattering coefficient, upper right panel ammonium *vs.* the scatter coefficient, lower left panel total organics *vs*. the scatter coefficient, lower right panel nitrate *vs*. the scatter coefficient, lower panel sulfate *vs.* the scatter coefficient.

Scattering coefficient and POA are dependent on both days with r^2 of 0.87 and 0.55 respectively (Fig. 4, middle panel, for second day not shown), when no

correlation with SOA has been observed, low values of r^2 being retrieved (0.07 and 0.006 respectively) (Fig. 4, middle panels).

The resulting solution, from positive matrix factorisation, for two factors, was properly evaluated, SOA being better correlated with SO_4.

Low correlation between SO_4 concentrations and scattering coefficients were found (Fig. 4, panel lower panel). These suggest that the sulphate aerosols fraction have another origin since the time series evolution of SO_4 had a different pattern than the other chemical species. The most probable source of SO_4 is long range transport which has a more regional character than the other species. SO_4 was found to be correlated with low-volatility oxygenated organic aerosol (LV-OOA) for typical long range transported aerosol [35] and in this specific event with highly processed aerosols.

Compared with other studies, sulphate as $(NH_4)_2SO_4$ has a lower contribution to light scattering [8]. While chloride, seems to be an important inorganic fraction that contribute to scatter coefficient, but not sufficient evidenced are found in previous studies. The presence of a relatively high concentration of chloride, with a maximum peak of 2 μg/m^3 was unusual for this region where the average is around 0.1 μg/m^3 [28] and together with *m*/*z* 57 emphasise the presence of plastics in the fire [36].

Another detailed analyses on organic fractions was proceed for *m*/*z* 43 and 57, scattering coefficient being 0.98 higher than total POA (Fig. 4, middle left panel). The abundance of *m*/*z 57* ($C_4H_9^+$) was associated with primary organic aerosol as Canagaratna *et al.* [32] has shown. According to Adler *et al.* (2011) and He *et al.* (2010) *m*/*z* 57 is related to hydrocarbon compounds or long alkyl chains. Values of the percentage of the *m*/*z* 57 from the total organic signal (slope of Δ*m*/*z*57/Δorg) higher than 0.06, are associated with vehicle exhaust or plastic burning aerosols. In this study, the values were between 0.096 and 0.073 (Figs. 5 and 6).

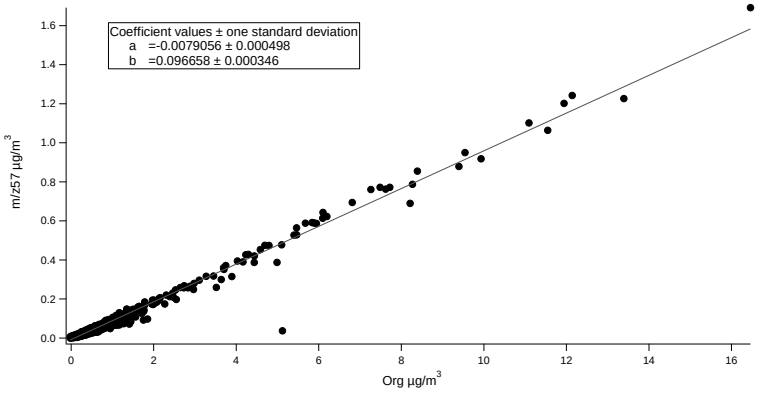

Fig. 5 – *m*/*z* 57 *vs*. total organics 27.04.2010.

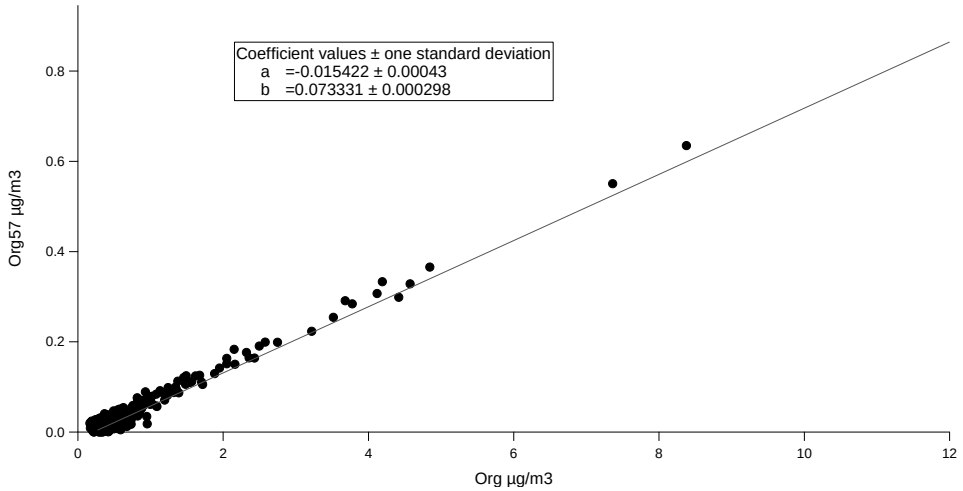

Fig. 6 – *m*/*z* 57 *vs.* total organics 28.04.2010.

Another high contribution to light scattering is chloride and ammonia that has an r^2 with scattering coefficient of 0.8226 and 0.8214 respectively. These two chemical species are internally mixed to ammonium chloride, having a correlation of 0.98 (not shown), possibly as a result of the burning process. Most likely the local fire sources were mixed with some domestic waste including plastics.

Unimodal non-refractory submicronic aerosols size distributions centred on 300 nm (Fig. 7, upper panel), were observed during the local fire event. During the second day (Fig. 7, lower panel) particle sizes are larger, up to 700 nm. This pattern is characteristic for hydrocarbon-like organic aerosols (HOA), the aging process being evident by the presence of larger particles. These results are in accordance with recent studies [8], which demonstrate that the highest contributions to light scattering are submicron particles.

The Angstrom exponent during local fire episode was 1.45 ± 0.05 emphasizing the presence of small particles. The average values of 1.35 ± 0.03 are characteristic for the next day, specific for fine particles as well. During the second day the concentration of aerosols was very low (under 1 µg/m^3). The primary aerosols were present in the data in lower proportion, while the secondary aerosols with a clearly oxidised pattern were detected (Fig. 7, lower panel). In this case the correlations between the AMS data and the Nephelometer data, for chemical species, were different. A higher correlation was observed for NH_4, Chl and NO_3 with a value of 0.85, 0.76 and 0.72 respectively and total organics decreased to 0.61.

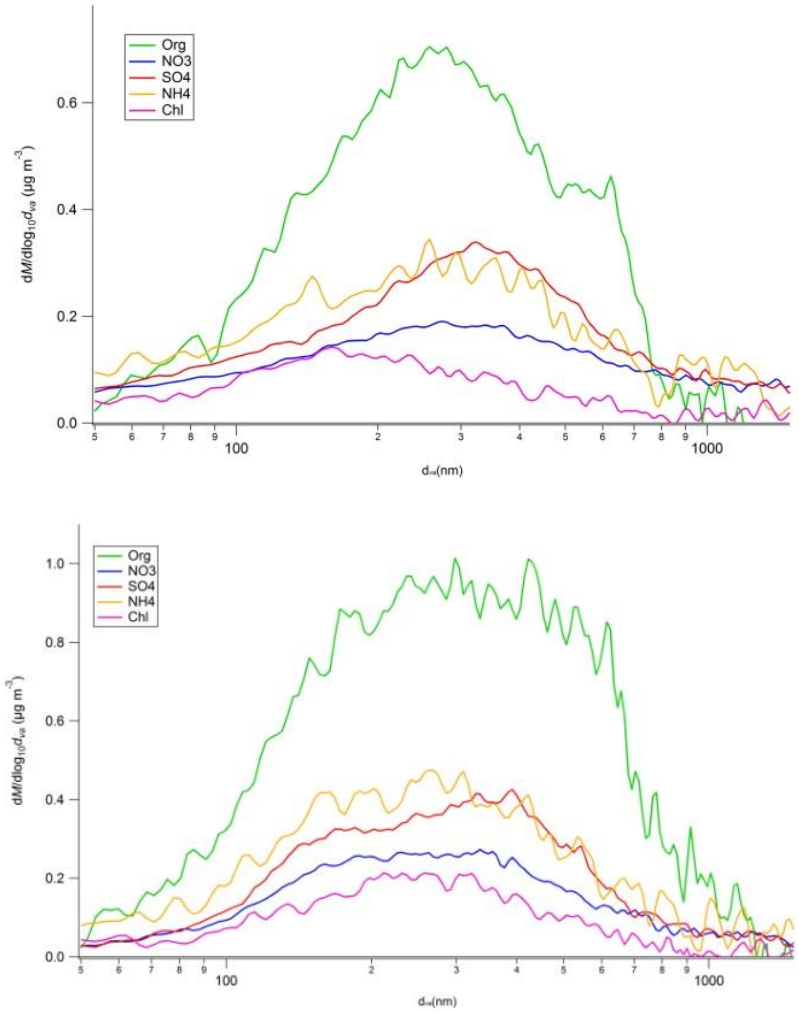

Fig. 7 – Size distribution of aerosols: upper panel 27.04.2010, lower panel 28.04.2010.

4. CONCLUSIONS

The study was conducted in Măgurele, a city close to Bucharest, Romania, when atmospheric aerosol loadings were significant. Aerosol sources were highlighted through analysis of submicronic non-refractory particles using an AMS and the scattering coefficient using a Nephelometer. The organic components are one of the main contributors to light scattering. The degree of oxidation of organics highly influence the scattering, in first day and in second day POA being correlated with scatter coefficient, since for SOA correlation was absent.

Some organic ion fragments (*m*/*z* 44, 43, 55, 57) were closely studied along with the scatter coefficient. The relation between *m*/*z* 57, 43 and the scatter coefficient was assessed for local fire case. We found high correlation factors (0.98), which pinpointed the same aerosol source. The aging phases were examined during the second day of measurements where correlation of the scatter coefficient and total organics decreased to 0.61.

During the local fire event we found that the organic component was dominated by the hydrocarbon signatures spectrum, with the ion series $C_nH^+_{2n+1}$ and $C_nH^+_{2n-1}$ (*m*/*z* 27, 41, 43, 55, 57, 69, 71...).

Ammonium Chloride aerosol highly influences the scatter coefficient in the special condition when its formation is favorited by high chloride concentration in the atmosphere. Similar behaviour of chloride and ammonium (r^2 = 0.82 for both ions) detected in the aerosol shows that they were internally mixed to ammonium chloride. The low correlation of SO_4 (r^2 = 0.46) with the scattering coefficient can be attributed to another source like long range transport.

The size distribution analyses revealed particles ranging from 200 to 700 nm. The bimodal distribution on the second day of the local fire case highlighted the aging process of aerosols emitted on the previous day.

Acknowledgements. This work was supported: by the Romanian-Swiss Research Programme, project number IZERZO_142146/1; by the Romanian National Authority for Scientific Research-PNCDI II, project number 309/2014 MOBBE.

REFERENCES

1. S. Stefan, Atmospheric aerosol physics, Ed. All, Bucuresti, 1998.
2. A. K. Pratt, K. A. Prathe, Mass Spectrom Rev., **31**(1), 17-48, doi: 10.1002/mas.20330, 2011.
3. T.F., D. Qin, G.-K. Plattner, M. Tignor, S.K. Allen, J. Boschung, A. Nauels, Y. Xia, V. Bex and P.M. Midgley (eds.), IPCC, Clouds and Aerosols. In: Climate Change 2013: The Physical Science Basis. Stocker, Cambridge University Press, Cambridge, United Kingdom and New York, NY, USA, 2013.
4. M. Crippa, P. F. DeCarlo, J. Slowik, C. Mohr, M. F. Heringa, R. Chirico, L. Poulain, F. Freutel, J. Sciare, J. Cozic, C. F. Di Marco, M. Elsasser, J. B. Nicolas, N. Marchand, E. Abidi, A. Wiedensohler, F. Drewnick, J. Schneider, S. Borrmann, E. Nemitz, R. Zimmermann, J.-L. Jaffrezo, A. S. H. Prévôt, U. Baltensperger, Atmos. Chem. Phys. 13, 961-981, 2013.
5. T.C. Bond, R.W. Bergstrom, Aerosol Sci. Tech. **40**, 27-67, doi:10.1080/02786820500421521, 2006.
6. B.J. Finlayson-Pitts, J.N.Jr. Pitts, *Chemistry of the Upper and Lower Atmosphere: Theory, Experiments, and Applications*, Academic Press, San Diego, 2000.
7. Schuster, G. L., O. Dubovik, and B. N. Holben, Angstrom exponent and bimodal aerosol size distributions, J. Geophys. Res., 111, D07207, doi:10.1029/2005JD006328 (2006).
8. J. Taoa, Leiming Z., J. Gaoa, H. Wang, F, Chai, S. Wanga, Atmospheric Environment 110, pp. 36-44, doi:10.1016/j.atmosenv.2015.03.037, 2015.
9. G. Paredes-Miranda, P. Arnott, J. Jimenez-Palacios, A.C. Aiken, J.S. Gaffney, N.A. Marley, Atmos. Chem. Phys., 9, 3721-3730. doi:10.5194/acp-9-3721-2009, 2009.

10. Q. Chen, Farmer, D.K., Rizzo, L.V., Pauliquevis, T., Kuwata, M., Karl, T.G., Guenther, A., Allan, J.D., Coe, H., Andreae, M.O., Pöschl, U., Jimenez, J.L., Artaxo, P., and Martin, S.T., Atmos. Chem. Phys. Discuss. 14, 16151–16186. doi:10.5194/acpd-14-16151-2014, 2014.
11. A. Nemuc, I.S. Stachlewska, J. Vasilescu, J.A. Górska, D. Nicolae, C. Talianu, ACTA GEOPHYS, **62**(2), 350-366, 10.2478/s11600-013-0180-7, 2013.
12. A.I. Calvo, C. Alves, A. Castro, V. Pont, A.M. Vicente, R. Fraile, Atmospheric Research 120–121, 1-28. doi: 10.1016/j.atmosres.2012.09.021, 2013.
13. Toanca Florica, Sabina Stefan, Temporal variability of atmospheric aerosols (PM10) in Magurele during 2006 and 2007, Book of abstracts, Annual Scientific Conference, Bucharest, Romania, 30-31, 2012.
14. A. Pietruczuk, J. Jarosławski, Acta Geophysica, **61(2)**, 445-462, doi: 10.2478/s11600-012-0069-x, 2013.
15. F. Drewnick, S.S. Hings, M.R. Alfarra, A.S.H. Prevot, S. Borrmann, Atmospheric Measurement Techniques. **2**:33-46, 2009.
16. T. Muller, M. Laborde, G. Kassell and A. Wiedensohler, Atmos. Meas. Tech., **4**, 1291-1303, 2011.
17. J.L. Jimenez, J.T. Jayne, Q. Shi, C.E. Kolb, D.R. Worsnop, I. Yourshaw, J.H. Seinfeld, R.C. Flagan, X. Zhang, K.A. Smith, J. Morris, P. Davidovits, Journal of Geophysical Research, **108 (D7)**, 8425-8438. doi:10.1029/2001JD001213, 2003.
18. P.F. DeCarlo, J.R. Kimmel, A. Trimborn, M.J. Northway, J.T. Jayne, A.C. Aiken, M. Gonin, K. Fuhrer, T. Horvath, K.S. Docherty, D.R. Worsnop, J.L. Jimenez,. Anal Chem **78**:8281-8289, 2006.
19. F. Freutel, J. Schneider, F. Drewnick, S.-L. von der Weiden-Reinmuller, M. Crippa, A.S.H. Prevot, U. Baltensperger, L. Poulain, A. Wiedensohler, J. Sciare, R. Sarda-Esteve, J. F. Burkhart, S. Eckhardt, A. Stohl, V. Gros, A. Colomb, V. Michoud, J. F. Doussin, A. Borbon, M. Haeffelin, Y. Morille, M. Beekmann, and S. Borrmann, Atmos. Chem. Phys. **13**, 933-959, 2013.
20. A. Zelenyuk, D. Imre, Y. Cai, K. Mueller, Y. Han, P. Imrich, Int. J. Mass Spectrom. **258**, 58-73, 2006.
21. A.C. Targino, K.J. Noone, E. Öström, Tellus **57B (3)**, 247-260. doi:10.1111/j.1600-0889.2005.00147.x., 2005.
22. A. D. McNaught and A. Wilkinson. Blackwell Scientific Publications, Oxford (1997). XML on-line corrected version: http://goldbook.iupac.org created by M. Nic, J. Jirat, B. Kosata; updates compiled by A. Jenkins.IUPAC. (2006), Compendium of Chemical Terminology, 2nd ed., doi:10.1351/goldbook. Last update: 2012-08-19; version: 2.3.2.DOI of this term: doi:10.1351/goldbook. M03752, 2006.
23. J. Vasilescu, A. Nemuc, L. Marmureanu, D. Nicolae, Environmental Engineering and Management Journal, **10**(1), 121-126, 2011.
24. P. Paatero, P. K. J. Hopke, Chemometrics, **23**, 91-100, 2009.
25. F. Canonaco, M. Crippa, J. G.Slowik, U. Baltensperger, and A.S.H. Prévôt., Atmos. Meas. Tech., **6**, 3649-3661, 2013.
26. Mihai *et al*., Journal of Atmospheric and Oceanic Technology **28(10**), 1307-1316. DOI: 10.1175/2011JTECHA1532.1, 2011.
27. V.A. Kovalev, W.E. Eichinger, Elastic Lidar: Theory, Practice, and Analysis Methods, 1st ed. John Wiley & Sons, Hoboken, New Jersey, 2004.
28. J. Vasilescu, L. Marmureanu, A. Nemuc, D. Nicolae, C. Talianu, *Seasonal variation of the aerosol chemical composition in a Romanian peri-urban area*, Environmental Engineering and Management Journal-accepted, 2012.
29. A. Bigi, G. Ghermandi, R. M. Harrison, J. Environ. Monit., 14, 552-563, 2012.
30. M.L. McGuire, *et al.*, Atmos. Chem. Phys. **14**, 8017-8042, 2014.
31. J.G. Slowik, A. Vlasenko, M. Mcguire, G.J. Evans, J.P.D. Abbatt, Atmospheric Chemistry and Physics. **10**, 1969-1988, 2010.

32. M.R. Canagaratna, J.T. Jayne, J.L. Jimenez, J.D. Allan, M.R. Alfarra, Q. Zhang, T.B. Onasch, F. Drewnick, H. Coe, A. Middlebrook, A. Delia, L.R. Williams, A.M. Trimborn, M.J. Northway, P.F. DeCarlo, C.E. Kolb, P. Davidovits, D.R. Worsnop, Mass Spectrometry Reviews. **26**, 185-222. doi 10.1002/mas.20115, 2007.
33. M.J. Cubison, A.M. Ortega, P.L. Hayes, D.K. Farmer, D. Day, M.J. Lechner, W.H. Brune, E. Apel, G.S. Diskin, *et al*., Atmospheric Chemistry and Physics. **11**, 12049-12064, doi:10.5194/acp-11-12049-2011, 2011.
34. G. Adler, J.M. Flores, A. A. Riziq, S. Borrmann, Y. Rudich, Atmospheric Chemistry and Physics, **11**, 1491-1503. doi:10.5194/acp-11-1491-2011, 2011.
35. P.F. DeCarlo, I.M. Ulbrich, J. Crounse, B. Foy, E.J. Dunlea, A.C. Aiken, D. Knapp, A.J. Weinheimer, T. Campos, P.O. Wennberg, J.L. Jimenez, Atmospheric Chemistry and Physics. **10**, 5257-5280, doi:10.5194/acp-10-5257-2010, 2010.
36. L-Y. He, Y. Lin, X.-F. Huang, S. Guo, L. Xue, Q. Su, M. Hu, S.-J. Luan, Y.-H. Zhang, Atmospheric Chemistry and Physics, **10 (23)**, 11535-11543. doi:10.5194/acp-10-11535-2010, 2010.